

Performance Analysis of Thermographic Cameras Applied to Wood Damage Detection

António Costa ^{a*}, Rui Pitarma ^a

^a Polytechnic Institute of Guarda, Guarda, Portugal

Abstract

Wood is a crucial component of the green economy of the 21st Century. From house construction to innovative daily applications and products, wood is one of the most sustainable resources. However, as a natural material, it suffers deterioration with time. Infrared thermography may provide an excellent potential for detecting internal damage. Although the prices of infrared cameras have dropped recently, getting the best value for money and choosing the right camera for wood inspection is a significant challenge. Before choosing an infrared camera, the operator needs to consider several parameters, such as the temperature range, spectral range, thermal sensitivity, resolution, spatial resolution, accuracy, optics and focus, to make an informed decision. This study aims to evaluate the performance of two infrared cameras, a high-end model and a mid-range model, in visual wood damage detection. For this purpose, samples of different wood species with induced damage were observed using active thermography. Our results suggest that, for technical purposes such as qualitative studies, resolution and thermal sensitivity may be more important parameters than accuracy. The results achieved are an important contribution when deciding which infrared camera to purchase.

Keywords: *Infrared Cameras, Thermal Sensitivity, Resolution, Accuracy, Performance, Wood Damage Detection*

1. Introduction

The exponential increase in population poses challenges to housing as the ecological footprint is significant. Building materials with mineral or metallic mineral origin contribute to the greenhouse effect. This reality forces a necessary and urgent reinvention of conventional housing for more highly efficient and widely applicable sustainable materials [1]. Wood is a renewable material that can contribute to sustainability [2]. It is renewable, and its CO₂-storing character has brought it into the focus of sustainable development [3].

The use of wood has the advantage of contributing to reducing greenhouse gases, as the tree binds carbon dioxide during its growth and retains it even after the tree has been felled, only releasing it again when it is burnt [3]. One cubic meter of tree

growth consumes 1 ton of carbon dioxide and releases 0.7 ton of oxygen [4]. Like other building materials, wooden structures are susceptible to biological attacks. Fungi and insects are the main organisms that can decompose wood and cause damage to structures. Therefore, monitoring systems are crucial to detect anomalies at an early stage and thus reduce maintenance and repair costs.

In this sense, infrared thermography (IRT) is a technique suitable for wood diagnosis, as it is a non-invasive and non-destructive inspection technique that allows the visualization of the entire structure and location of internal defects. This technique enables the superficial temperature of the objects to be visualized; it is based on the radiation emitted by the object. Thermography results from a complex interaction between the heat source, the material, and its defects [5].

* Corresponding author. Tel.: +351 271 220 100

Fax: +351 271 222 690; E-mail: antoniocosta@ipg.pt

© 2016 International Association for Sharing Knowledge and Sustainability

DOI: 10.5383/ijtee.19.02.001

In recent decades, IRT has become a technology with multiple applications, such as non-destructive testing, condition monitoring, predictive maintenance, and reducing the energy costs of processes and buildings. The proliferation of IRT technology is partly due to the development and the minimal instrumentation required to use them, which are a tripod or camera stand, and a video output device to display the captured infrared thermal images (TI) [6,7]. IRT is a comprehensive and non-hazardous technique for acquiring and processing thermal information from non-contact measuring devices [7–11]. As a non-contact technique, thermography is extremely effective, safe, and simple. IRT allows the temperature of objects to be determined based on the radiation emitted [11–13] using an infrared (IR) camera.

All objects with a temperature above absolute zero emit radiation in the electromagnetic spectrum at the infrared wavelength. IRT detects radiation in the infrared spectrum, usually between 2.0 and 5.6 μm and 8.0 and 14.0 μm because these spectral windows present poor atmospheric absorption [5]. The detected radiation is converted into electronic signals and then transformed into a thermal image. To highlight details in TI, the surfaces of the objects must have different temperatures. IRT technology can create this thermal gradient on the surface through two thermographic procedures: passive and active. In the passive procedure, the thermal contrast is generated by a natural source such as sunlight [14]. When a natural source is not sufficient to create a thermal contrast between the object and the background, an active thermography (AT) procedure is required. AT uses an external energy source to create an energy stimulus on the object under investigation, which causes an internal heat flux on the surface of the object [11,15,16]. AT can be performed using two methods - transmissive thermography and reflected thermography - depending on the relative position of the heat sources and the IRC camera. In transmissive thermography, thermal excitation is applied to the surface opposite the surface in the IRC's field of view (FOV). In reflected thermography, thermal excitation is applied directly to the surface in the IRC's FOV [6,17]. The generated heat flow is disturbed if defects or damage on or near the elements surface to be analyzed cause a discontinuity/ thermal contrast, which is detected by analyzing the thermograms obtained [18].

When the IR camera is pointed at an object, the camera receives radiation from the object itself, from the reflection of radiation on the object due to emissions from surrounding bodies, and from radiation emitted by the atmosphere. The IR camera captures this radiation and creates a thermographic image (TI) visible to the human eye. The thermal image produced by an IR camera (also known as a thermogram) is represented by a thermal color code, in the form of a color gradient based on the highest or lowest temperature captured throughout its FOV, taking into account the maximum and minimum temperatures selected during the configuration of the equipment [19–21].

Like any other technical system, the use of an IR camera requires practice and basic knowledge by the operator. As previously noted, the core purpose of an IR camera is to convert IR radiation into a visual image. The two-dimensional distribution of IR radiation generated by an object or scene should be represented by the visual image [22]. The main components of an IR camera are the optics, the detector, the cooling or temperature stabilization of the detector, the electronics for signal and image processing, and the image display [Fig. 1].

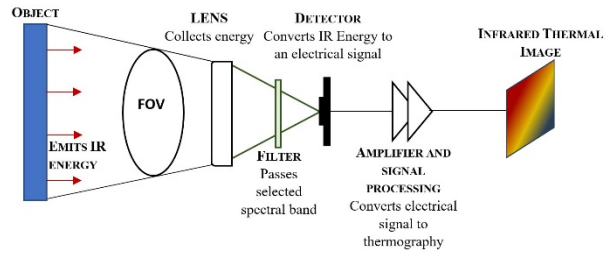


Fig. 1. Schematic diagram of infrared thermography camera. Adapted from [23].

The design of the optical mechanism used to visualize thermographic images is the same as that of the optical system for wavelengths in the visible range, only the materials used are different. The thermal detector is the most important part of the thermographic camera. It determines the thermal sensitivity and the spatial resolution that can be achieved. Several parameters need to be considered before choosing an infrared camera, such as the temperature range, spectral range, thermal sensitivity, resolution, spatial resolution, accuracy, optics, and focus. A detailed study of these performance parameters of thermal imaging systems is reported by [24]. Some important parameters are mentioned below:

Resolution: The resolution of the thermal camera sensor determines the quality of the rendered image. The resolution indicates the number of pixels in the detector. More pixels mean a higher resolution. The higher the resolution of the detector, the sharper and more accurate each individual point in the image will be, allowing for more precise measurements and better decisions. Higher resolution infrared cameras can measure smaller targets at a greater distance and create sharper TI for more accurate and reliable measurements.

Spatial resolution: The spatial resolution of a thermal imaging system is defined as the ability of the camera to distinguish between two objects within the FOV. The FOV is determined by the camera lens and refers to the extent of the scene that the camera can capture. The greater the FOV, the greater the area or space that can be captured with the thermal camera. Some cameras are available with multiple lenses for different types of applications.

Thermal sensitivity: The thermal sensitivity is equivalent to the smallest difference in temperature that the camera is able to measure without being attributed to its own noise. Devices with higher thermal sensitivity can detect slight temperature differences and therefore provide more detailed thermograms. The temperature resolution and the spatial resolution are important performance parameters, as they significantly influence the image quality [22].

Accuracy: All measurements are subject to error and, temperature measurements with thermography are unfortunately no exception. Therefore, it is important to know the accuracy of the IR cameras. The accuracy specification gives the absolute value of the temperature measurement error for blackbody temperature measurements [16,24].

In addition to the above performance parameters, the selection of an IR camera also depends on inherent parameters such as the size, weight, image processing capabilities, calibration, storage capacity, computer interface, cost, and service. In any practical thermal imaging application, the operator must ultimately answer the following question: *Based on its performance*

parameters, is the camera suitable for my application? Accurate knowledge of the main performance limits of the thermal imaging system used and their relevance to the application is crucial for the correct interpretation of the results focusing on professional and research and development environments.

The aim of this study is to evaluate and compare the performance of two IR cameras, a high-end and a mid-range model, applied to the detection of wood damage. The high-end and mid-range models have better resolution, more precision and higher thermal sensitivity and are far more expensive compared to low-cost IR sensor cameras. On the other hand, most advanced IR cameras offer numerous features and options compared to the low-cost IR sensor cameras. Unlike low-cost IR sensor cameras, the high-end and mid-range models have more software tools that allow the operator to control more performance parameters of the IR camera and thus improve the quality of the results obtained, as with the high-end and mid-range models used in professional and research and development environments. To evaluate the performance of these two cameras, samples of two wood species (*Pinus pinaster* and *Quercus faginea Lam*) were investigated using AT. Holes with different diameters and depths were drilled into these samples to simulate damage. The rest of the paper is structured as follows: methods, materials and the experimental setup are summarized in Section 2; Section 3 reports the experimental results and the comparison of the performance of the two IR cameras in detecting and identifying wood damage; conclusions are presented in Section 4.

2. Materials and Methods

2.1. Equipment

Two infrared cameras, a high-end model - FLIR T1030sc, and a mid-range model - FLIR ThermaCAM B20, were tested in visual wood damage detection [Fig. 2].



Fig. 2. Infrared cameras used in the experiments: FLIR T1030sc (high-end model) and FLIR ThermaCAM B20 (mid-range model).

Table 1 contains a brief comparison of the two IR cameras tested. The specifications are provided by the manufacturer [25,26].

Table 1. Main specifications for FLIR T1030sc and FLIR ThermaCAM B20 [25,26]

	FLIR T1030sc	FLIR ThermaCAM B20
IR sensor	1024 x 768 pixels	320 x 240 pixels
Thermal sensitivity	< 20 mK at 30°C	< 100 mK at 30°C
Minimum focus distance	0.4 m (standard lens)	0.50 (standard lens)
Spatial resolution	0.47 mrad (standard lens)	1.30 mrad (standard lens)
Spectral range	7.5 – 14 μm	7.5 – 13 μm
Accuracy	±1°C or ±1% at 25°C for temperatures between 5°C to 150°C. ±2°C or ±2% of reading at 25°C for temperatures up to 1200°C	±2°C or ±2% of reading

A FLIR MR 176 thermo-hygrometer was used to measure the laboratory conditions (relative humidity and ambient temperature), and sample moisture. The mass of the sample was measured using a KERN EMB balance.

2.2. Samples

For the experiments, wood samples from two species with different densities were used: *Pinus pinaster* and *Quercus faginea Lam* [Table 2]. The wood samples were used without any type of finishing, such as in many wood constructions and structures.

Table 2. Dimensions and physical properties of the wood samples.

	<i>Pinus pinaster</i>	<i>Quercus faginea Lam</i>
Length / (x10 ⁻³ m)	200.0±0.5	200.0±0.5
Width / (x10 ⁻³ m)	150.0±0.5	150.0±0.5
Thickness / (x10 ⁻³ m)	35.0±0.5	35.0±0.5
Mass / (x10 ⁻³ kg)	607±1	733±1
Volume / (x10 ⁻⁴ m ³)	9.6	9.6
Moisture / %	7.1±1.5	8.9±1.5
Density / (x10 ² kg.m ⁻³)	6.3	7.6

Wood is susceptible to diseases that shorten its useful life and reduce its durability. To analyze the performance of these two IR cameras, six holes (with different diameters and depths) were drilled into the wood to simulate damage [Table 3].

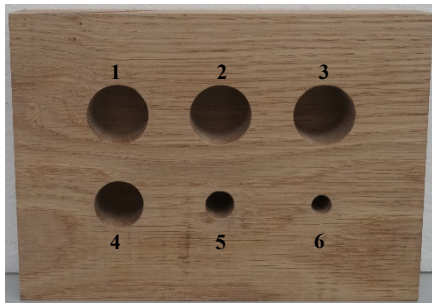
Table 3. Diameter and depth of the six holes induced on the back of the observed surface.

Induced hole	Diameter / ($\times 10^{-3}$ m)	Depth / ($\times 10^{-3}$ m)
1	30.0±0.5	29.0±0.5
2		31.5±0.5
3		33.0±0.5
4	24.5±0.5	33.0±0.5
5	14.5±0.5	
6	10.0±0.5	

These six induced holes were made on the side of the wood opposite to the observed surface [Fig. 3(b)].



(a)



(b)

Fig. 3. Example of a wood sample used in the experiments: (a) front view and (b) back view (numbers indicate the induced holes).

2.3. Methods

To obtain an accurate TI, parameters such as the emissivity of the sample, the reflected apparent temperature from the environment, the ambient temperature, the relative humidity of the environment and the distance between the sample and the IR camera must be entered into the device as input data [1]. The emissivity of the sample was measured using the Thermogram Analysis Method [10,27–29]. The reflected apparent temperature was measured using the aluminum leaf method [10,28,30]. Thermal contrast was required between the surface temperature and room temperature. The samples were heated by a radiant heating system. This system consists of two halogen heaters, each with a power of 1200 W, placed at an angle of 35° to the samples and on the same side as the IR cameras [Fig. 4].

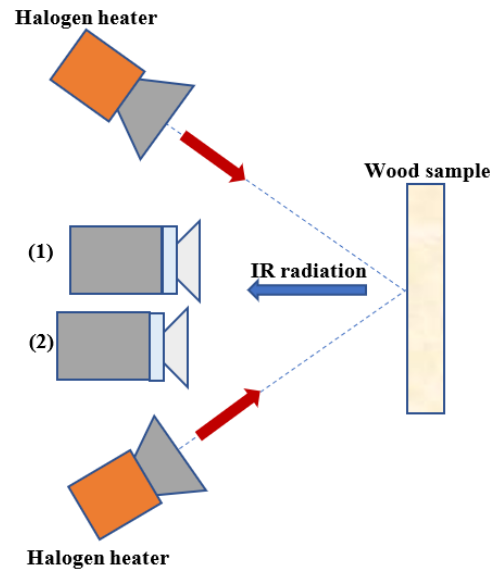


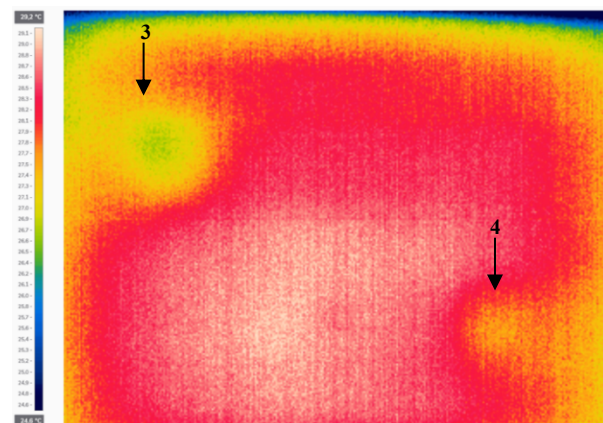
Fig. 4. Schematic representation of a radiant heating system. The IR cameras – (1) FLIR T130sc and (2) FLIR ThermoCAM B20 were placed side-by-side. Adapted from [31].

The two IR cameras were placed side by side but at 0.50 m (FLIR ThermoCAM B20) and 0.40 m (FLIR T130sc) from the wood sample to ensure the FOV of the lens [Fig.4]. The experiments were conducted following the active thermography procedure suggested by Costa and Pitarma [32]. As suggested by Costa and Pitarma [21], the thermograms were analyzed using the *Rainbow* color palette from FLIR Thermal Studio Suite software.

3. Results

The performance of the two IR cameras in detecting wood damage was analyzed by comparing the TI produced with the two cameras.

Figures 5 and 6 show TI taken by the FLIR ThermoCAM B20 [Fig. 5(a) and Fig. 6(a)] and the FLIR T130sc [Fig. 5(b) and 6(b)] of the *Pinus pinaster* sample.



(a)

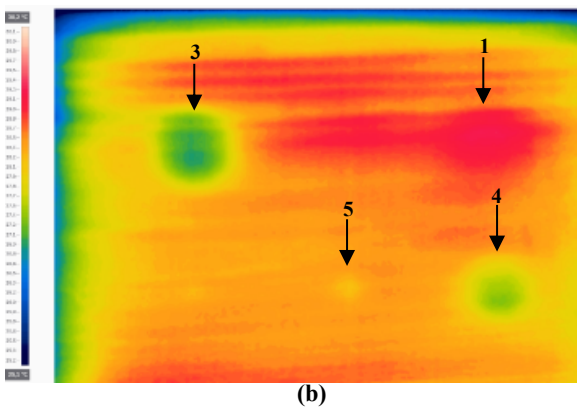


Fig. 5. Thermal images of a wood sample of *Pinus pinaster* taken with: (a) FLIR ThermaCAM B20 and (b) FLIR T1030sc. The numbers 1, 3–5 indicate the respective induced holes.

In Fig. 5(a), only induced holes 3 and 4 are visible. In Fig. 5(b), in addition to induced holes 3 and 4, induced holes 1 and 5 are also visible, with the details of the latter two being very distinct. In Fig. 5(b), the level of detail of induced holes 3 and 4 is higher than in TI of Fig. 5(a), so sharper contours can be seen.

The TI of Fig. 6(a) and 6(b) were taken after the TI of Fig. 5(a) and 5(b).

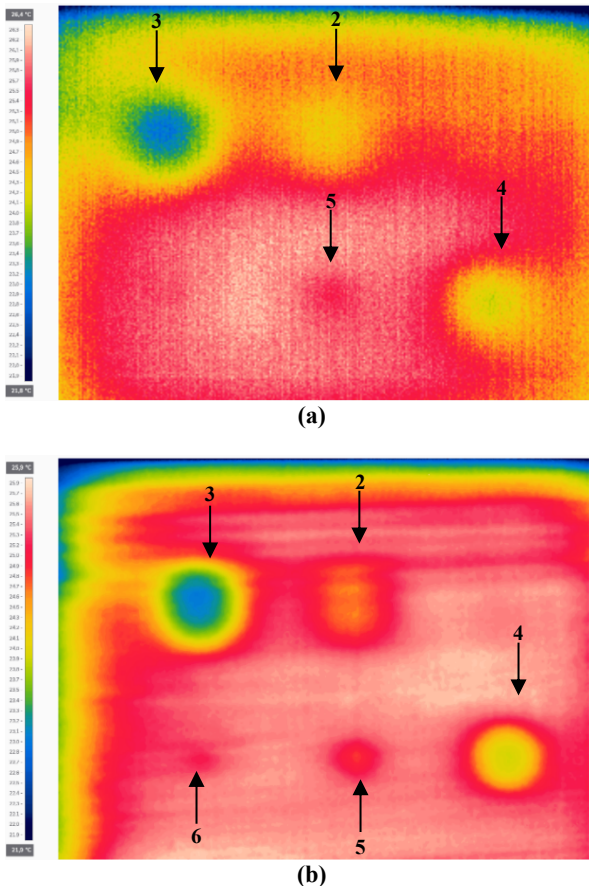


Fig. 6. Thermal images of a wood sample of *Pinus pinaster* taken with: (a) FLIR ThermaCAM B20 and (b) FLIR T1030sc. Numbers 2–6 identify the respective induced holes.

In TI of Fig. 6(a) and 6(b), more induced holes can be observed than in TI of Fig. 5(a) and 5(b). In Fig. 6(a) the induced holes 2–5 can be seen. In TI of Fig. 6(b), in addition to the induced holes 2–5, induced hole 6 (with a smaller diameter) can also be seen. Induced hole 1 (farther from the surface) is not visible in the two thermograms. The contours at induced holes 4 and 6 are more detailed in Fig. 6(a) and 6(b) than in TI in Fig. 5(a) and 5(b). Induced hole 4 is visible in both TI, but the level of detail is not very pronounced, and the contour of the induced hole is unclear in the two thermograms.

Figures 7 and 8 show TI taken by the FLIR ThermaCAM B20 [Fig. 7(a) and Fig. 8(a)] and the FLIR T1030sc (Fig. 7(b) and Fig. 8(b)) for the *Quercus faginea Lam* sample.

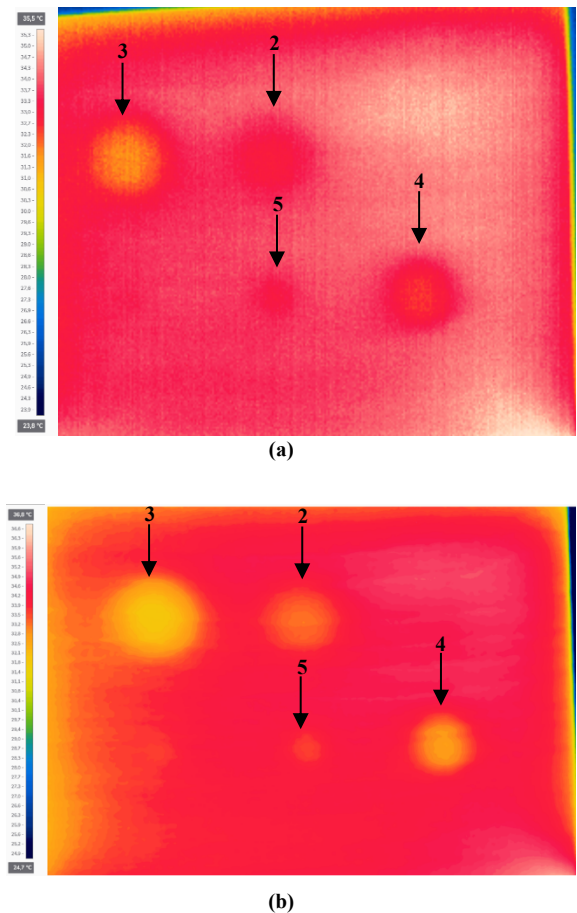


Fig. 7. Thermal images of a wood sample of *Quercus faginea Lam* taken with: (a) FLIR ThermaCAM B20 and (b) FLIR T1030sc. Numbers 2–5 identify the respective induced holes.

Figures 7(a) and 7(b) show induced holes 2–5. Although the same induced holes can be seen in both TI, the details are less pronounced in the thermogram recorded by the ThermaCAM B20. In thermogram 7(b), taken with the T1030sc, the level of detail of the induced holes is better than in thermogram 7(a), so sharper contours can be seen. Induced hole 1 (farther from the surface) and induced hole 6 (with a smaller diameter) cannot be detected regardless of the IR camera used.

The TI in Fig. 8(a) and 8(b) were captured after the TI of Fig. 7(a) and 7(b).

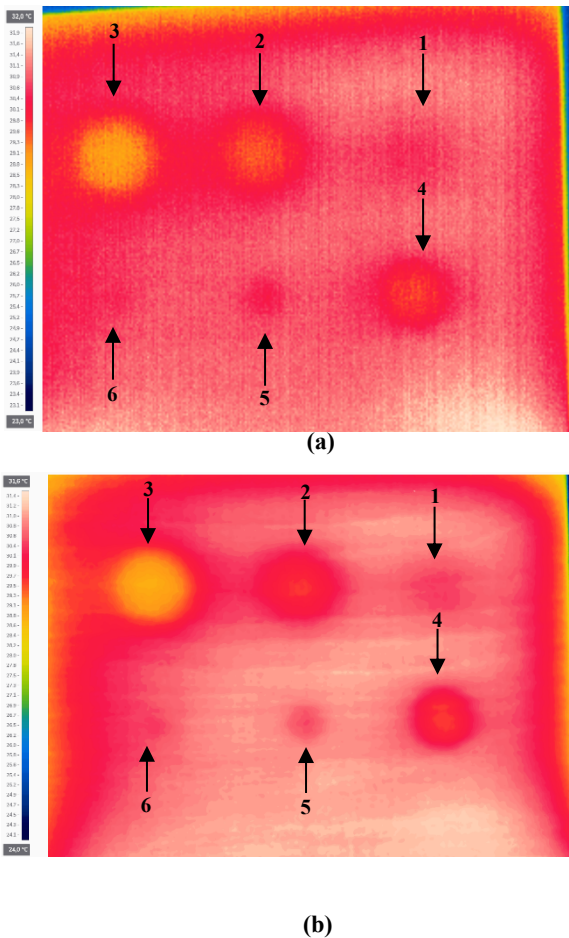


Fig. 8. Thermal images of a wood sample of *Quercus faginea* Lam taken with: (a) FLIR ThermoCAM B20 and (b) FLIR T1030sc. Numbers 1–6 identify the respective induced holes.

The TI in Fig. 8(a) and 8(b) show the induced damage 1, which is not visible in Fig. 7(a) and 7(b). All induced holes are visible in Fig. 8(a) and 8(b), but the level of detail is not very pronounced, and the contours of the induced holes are unclear in both thermograms. The contours at induced holes 3 and 2 are more detailed in Fig. 8(a) than in Fig. 7(a). The level of detail of the contours of the induced holes detected with the ThermoCAM B20 (Fig. 7(a) and 8(a)) is lower than the level of detail of the contours of the same induced holes detected with the T1030sc [Fig. 7(b) and 8(b)], corroborating the results obtained with the *Pinus pinaster* sample [32]. Note that in both cameras, the damage detection pattern for the *Pinus pinaster* sample is different than the detection pattern for the *Quercus faginea* Lam sample, with fewer induced holes detected in the *Pinus pinaster* sample, which may suggest the more the density of the wood, the better is the damage visualization.

Based on the results, higher-resolution IR cameras provide higher-quality TI, suggesting that the number of pixels is a crucial parameter in IR cameras. Thermal sensitivity is another variable that affects image quality. As the results show, an IR camera with low thermal sensitivity cannot differentiate close temperature values in areas that are less extended or have greater depth, and noise tends to dominate the image in this area, lowering the TI quality. In practices, wood damage inspection is characterized by qualitative analysis, so for the IR cameras, it is

more important to distinguish between two surface temperature points that are close to each other than to determine the temperatures at those points accurately.

4. Conclusions

Thermography is an excellent example of a visualization technique that can be used in many different fields such as non-destructive testing, condition monitoring, predictive maintenance, and reducing energy costs of processes and buildings. For some applications, the operator only needs infrared data represented as a visual image to interpret and identify the source of a problem. This qualitative method of thermography provides the visual cue necessary to act. Therefore, choosing the right camera is a challenge. The purposes of this research were to evaluate the performance of two infrared cameras, a high-end model and a mid-range model, in the visual detection of wood damage. Given the results, increasing the resolution of IR cameras provides better quality TI, allowing the conclusion that the number of pixels is a relevant parameter in IR cameras. Another parameter that affects image quality is thermal sensitivity. The results suggest that the IR cameras with low thermal sensitivity cannot distinguish between close temperature values in areas that are less extensive or have a greater depth. In these areas, noise starts to dominate the image and the quality of the thermograms consequently decreases. In qualitative studies, it is more important for the IR camera to be able to distinguish between two nearby surface temperature points than to measure the temperature of these points accurately. In this sense, the results suggest that the mid-range IR is suitable for visual detection when the damage to be detected is extensive or close to the surface, where higher resolution and thermal sensitivity are not required. However, for a less extensive area or the greatest depth, the use of a mid-range IR camera is not suitable, and a more advanced IR camera is needed. In this respect, an IR camera with higher resolution and thermal sensitivity provides more accurate qualitative results and has proven to be effective in detecting the finer details of wood damage. Our work underlines the idea that for technical purposes, i.e., for qualitative studies, resolution and thermal sensitivity may be more important parameters than accuracy.

References

- [1] Jiang F, Li T, Li Y, Zhang Y, Gong A, Dai J, et al. Wood-Based Nanotechnologies toward Sustainability. *Advanced Materials* 2018;30:1703453. DOI:10.1002/adma.201703453.
- [2] Blanchet P, Breton C. Wood Productions and Renewable Materials: The Future is Now. *Forests* 2020;11:657. DOI: 10.3390/f11060657.
- [3] Goldhahn C, Cabane E, Chanana M. Sustainability in wood materials science: an opinion about current material development techniques and the end of lifetime perspectives. *Phil Trans R Soc A* 2021;379:20200339.
- [4] Pitarma R, Crisóstomo J, Pereira L. Detection of wood damages using infrared thermography. *Procedia Computer Science* 2019;155:480–6. DOI:10.1016/j.procs.2019.08.067.
- [5] Silva ME, Dias A, Lousada JL. *Madeira de Pinho - Características e utilização*. Vila Real, Portugal: UTAD; 2013.
- [6] Maldague X. *Theory and practice of infrared technology for nondestructive testing*. New York: Wiley, 2001.

- [7] Bucur V. Nondestructive characterization and imaging of wood: with 49 tables. Berlin Heidelberg: Springer, 2003.
- [8] Bagavathiappan S, Lahiri BB, Saravanan T, Philip J, Jayakumar T. Infrared thermography for condition monitoring – A review. *Infrared Physics & Technology* 2013;60:35–55. DOI:10.1016/j.infrared.2013.03.006.
- [9] Pitarma R, Pereira L, Crisóstomo J. Infrared Thermography Applied to Inspection of Wood Damages. In: Ksibi M, Ghorbal A, Chakraborty S, Chaminé HI, Barbieri M, Guerriero G, et al. (Eds.), *Recent Advances in Environmental Science from the Euro-Mediterranean and Surrounding Regions* (2nd Edition), Cham: Springer International Publishing, 2021, pp. 2293–7. DOI:10.1007/978-3-030-51210-1_359.
- [10] Pitarma R, Crisóstomo J. An Approach Method to Evaluate Wood Emissivity. *Journal of Engineering* 2019;2019:1–9. DOI:10.1155/2019/4925056.
- [11] Pitarma R, Crisóstomo J. Inspection of Trees Using Infrared Thermography. In: Ksibi M, Ghorbal A, Chakraborty S, Chaminé HI, Barbieri M, Guerriero G, et al. (Eds.), *Recent Advances in Environmental Science from the Euro-Mediterranean and Surrounding Regions* (2nd Edition), Cham: Springer International Publishing; 2021, pp. 1507–12. DOI: 10.1007/978-3-030-51210-1_240.
- [12] Pitarma R, Crisóstomo J, Ferreira ME. Contribution to Trees Health Assessment Using Infrared Thermography. *Agriculture* 2019;9:171. DOI:10.3390/agriculture9080171.
- [13] Yao Y, Sfarra S, Lagüela S, Ibarra-Castanedo C, Wu J-Y, Maldague XPV, et al. Active thermography testing and data analysis for the state of conservation of panel paintings. *International Journal of Thermal Sciences* 2018;126:143–51. DOI:10.1016/j.ijthermalsci.2017.12.036.
- [14] Luo D, Wang S, Du X, Zhao P, Lu T, Yang H, et al. Health detection techniques for historic structures. *Materials Testing* 2021;63:855–64. https://doi.org/10.1515/mt-2021-0013.
- [15] Fronapfel E, Stolz B. Emissivity measurements of common construction materials. vol. 7, pp. 13–21.
- [16] Usamentiaga R, Venegas P, Guerediaga J, Vega L, Molleda J, Bulnes F. Infrared Thermography for Temperature Measurement and Non-Destructive Testing. *Sensors* 2014;14:12305–48. DOI:10.3390/s140712305.
- [17] Milovanović B, Banjad Pečur I. Review of Active IR Thermography for Detection and Characterization of Defects in Reinforced Concrete. *J Imaging* 2016;2:11. DOI:10.3390/jimaging2020011.
- [18] Benítez HD, Ibarra-Castanedo C, Bendada A, Maldague X, Loaiza H, Caicedo E. Definition of a new thermal contrast and pulse correction for defect quantification in pulsed thermography. *Infrared Physics & Technology* 2008;51:160–7. DOI:10.1016/j.infrared.2007.01.001.
- [19] Jadin MS, Taib S, Ghazali KH. Feature extraction and classification for detecting the thermal faults in electrical installations. *Measurement* 2014;57:15–24. DOI:10.1016/j.measurement.2014.07.010.
- [20] Cruz-Albarran IA, Benitez-Rangel JP, Osornio-Rios RA, Dominguez-Trejo B, Rodriguez-Medina DA, Morales-Hernandez LA. A new approach to obtain a colour palette in thermographic images. *Quantitative InfraRed Thermography Journal* 2019;16:35–54. DOI:10.1080/17686733.2018.1509199.
- [21] Costa A, Pitarma R. Performance Evaluation of Colour Codes on Thermal Image Analysis – Application in the Wood Damage Detection. *Lecture Notes in Networks and Systems*, Budva, Montenegro, 2022. DOI: 10.1007/978-3-031-04826-5_55
- [22] Venkataraman B, Raj B. Performance parameters for thermal imaging systems. *Insight - Non-Destructive Testing and Condition Monitoring* 2003;45:531–5. DOI:10.1784/insi.45.8.531.52914.
- [23] Jo YH, Lee CH, Yoo JH. Study on Applicability of Passive Infrared Thermography Analysis for Blistering Detection of Stone Cultural Heritage. *Journal of the Korean Conservation Science for Cultural Properties* 2013;29:55–67. DOI:10.12654/JCS.2013.29.1.06.
- [24] Vollmer M, Möllmann K-P. *Infrared thermal imaging: fundamentals, research and applications* (2nd edition), Weinheim, Germany: Wiley-VCH Verlag GmbH & Co. KGaA, 2018.
- [25] FLIR S. *ThermCAM B20 user’s manual*. Melrose, Massachusetts, 2008.
- [26] FLIR S. *FLIR T10XX series user’s manual*. Melrose, Massachusetts, 2017.
- [27] Pitarma R, Crisóstomo J, Jorge L. Analysis of Materials Emissivity Based on Image Software. In: Rocha Á, Correia AM, Adeli H, Reis LP, Mendonça Teixeira M. (Eds.), *New Advances in Information Systems and Technologies*, vol. 444, Cham: Springer International Publishing, 2016, pp. 749–57. DOI:10.1007/978-3-319-31232-3_70.
- [28] Pitarma R, Crisóstomo J. Determination of Wood Emissivity Using Active Infrared Thermography. In: Ksibi M, Ghorbal A, Chakraborty S, Chaminé HI, Barbieri M, Guerriero G, et al. (Eds.), *Recent Advances in Environmental Science from the Euro-Mediterranean and Surrounding Regions* (2nd Edition), Cham: Springer International Publishing, 2021, pp. 409–13. DOI:10.1007/978-3-030-51210-1_65.
- [29] Crisóstomo J, Pitarma R. The Importance of Emissivity on Monitoring and Conservation of Wooden Structures Using Infrared Thermography. In: Hassan M. (Ed.), *Advances in Structural Health Monitoring*, IntechOpen, 2019. DOI: 10.5772/intechopen.82847.
- [30] Mousavi M, Gandomi AH. Wood hole-damage detection and classification via contact ultrasonic testing. *Construction and Building Materials* 2021;307:124999. DOI: 10.1016/j.conbuildmat.2021.124999.
- [31] Crisostomo J. *Contribuição para a Análise de Manifestações Patológicas em Madeira na Construção com Recurso à termografia*. Master. Instituto Politécnico da Guarda, 2014.
- [32] Costa A, Pitarma R. Performance Evaluation Tests and Technical Relevant Parameters of Infrared Cameras for Contactless Wood Inspection. *Procedia Computer Science* 2022;203:318–25. DOI: 10.1016/j.procs.2022.07.040.